

Effect of dopant addition on oxygen sorption properties of La-Sr-Co-Fe-O perovskite type oxide

Qinghua Yin · Y. S. Lin

© Springer Science + Business Media, LLC 2006

Abstract The paper reports on effect of doping Ag^+ , Ni^{2+} , Ca^{2+} , Ba^{2+} or Zr^{4+} in $\text{La}_{0.1}\text{Sr}_{0.9}\text{Co}_{0.9}\text{Fe}_{0.1}\text{O}_{3-\delta}$ (LSCF1991) on its oxygen sorption capacity and desorption rate. The dopant can be incorporated into LSCF1991 matrix causing lattice expansion. The oxygen sorption capacity and tendency for the disordered perovskite to ordered brownmillerite phase transition for these samples decrease in the order: LSCF1991 > LSCF-Ag > LSCF-Ni > LSCF-Ca > LSCF-Ba > LSCF-Zr. The oxygen desorption rate also decreases in the same order for the doped samples. Doping increases the tendency of the disorder to order phase transition and enhances oxygen desorption rate during oxygen desorption step. Doping Ag and Ni provides more pronounced enhancement in oxygen desorption rate. The results suggest that Ag and Ni doped LSCF1991 samples are promising sorbents for use in a high temperature sorption process for air separation.

Keywords Air separation · Perovskite-type oxides · Phase transition · Kinetics · Oxygen sorption capacity

1 Introduction

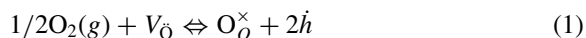
Oxygen and oxygen-enriched air are important for many industrial and medical applications (Kang et al.,

1996; Prasad, 1998; Dyer et al., 2000). For example, they can be used to improve the efficiencies of combustion processes and lead to a reduction in carbon monoxide or hydrocarbons in the exhausts. To obtain high purity oxygen in large scale, cryogenic air separation is the only commercially available method, which is known for its major drawback of high energy consumption. The replacements of the cryogenic air separation with other less energy consuming oxygen separation methods have been explored for many years. Recently a new high temperature air separation process with a perovskite-type metal oxide sorbent was proposed by Lin and co workers (Lin et al., 2000; Yang et al., 2002). The sorption separation process can be used to produce pure nitrogen and oxygen enriched air for various applications.

Perovskite-type oxides are a group of metal oxides having the general formula of ABO_3 . Oxygen nonstoichiometry (vacancy) occurs in some perovskite-type oxides with B-site cations of variable oxidation states and A-site cations partially substituted by another cation with lower oxidation state. Based on the fact that the oxygen nonstoichiometry in their structure varies with oxygen partial pressure of surrounding gas and temperature, these materials can be applied in pressure or temperature swing adsorption process for air separation. The new sorption process takes advantage of the unique properties of these perovskite-type oxides that can adsorb a large quantity of O_2 , but not other gases, into the oxygen vacancy site at high temperatures. The sorption and desorption mechanism is based

Q. Yin · Y. S. Lin (✉)
Department of Chemical Engineering, Arizona State
University, Tempe, AZ 85287-6006, USA
e-mail: Jerry.Lin@asu.edu

on the following reversible defect reaction (Mizusaki et al., 1984; Mizusaki et al., 1989):



where V_{O} , $\text{O}_{\text{O}}^{\times}$ and h denote positive oxygen vacancy, neutralized lattice oxygen and mobile electron hole, respectively. Infinitely high selectivity for oxygen over nitrogen and high oxygen adsorption amount are the major characteristics of this group of materials.

Lin and co workers performed a series of fundamental studies on perovskite-type oxides as sorbents, including selection and syntheses of materials (Yang et al., 2002), oxygen sorption equilibrium (Yang et al., 2002; Yang and Lin, 2003a), oxygen sorption thermal effects (Yang and Lin, 2005), and oxygen sorption and desorption kinetics as well as fixed-bed process performance (Yang and Lin, 2003b). To be a promising sorbent material for air separation, the perovskite-type oxide must have a high oxygen sorption capacity as well as a fast sorption/desorption rate in the sorption processes. Yang et al. (2002) reported that the perovskite-type oxide, $\text{La}_{0.1}\text{Sr}_{0.9}\text{Co}_{0.9}\text{Fe}_{0.1}\text{O}_{3-\delta}$ (LSCF1991), can adsorb oxygen up to 0.6 mmol/g with zero sorption for nitrogen, and the sorption rate in this process is also high. However, the oxygen desorption rate is slow in the temperature range of 400–900°C. This issue represents a major challenge with regards to achieving a high O_2 -product purity in the industrial application of air separation needed for many purposes, and also to ensuring a sufficiently high efficiency of sorbent regeneration.

Increasing the desorption rate is of great importance to develop the separation process with a perovskite type oxide sorbent for air separation. A common approach to improve the properties of perovskite type metal oxides is through addition of ion in the metal oxide. Kharton and co workers found that the oxygen surface exchange rate for $\text{La}_x\text{Sr}_{1-x}\text{CoFe}_{3-\delta}$ ($x = 0.1-0.3$) can be enhanced by doping a catalytically active metal ion such as Ag^+ or Ni^+ (Choudhary et al., 1999; Kharton et al., 2002; Figueiredo et al., 2004; Kharton et al., 2004). Tan et al. (2004a, b) reported that addition of Ag^+ into $\text{SrCo}_{0.8}\text{Fe}_{0.2}\text{O}_{3-\delta}$ membrane increased its oxygen permeation flux. Doping Ba^{2+} and Zr^{4+} into perovskite-type oxides can increase the membrane stability under reducing atmosphere (with low P_{O_2}) but decrease the oxygen permeation flux through these

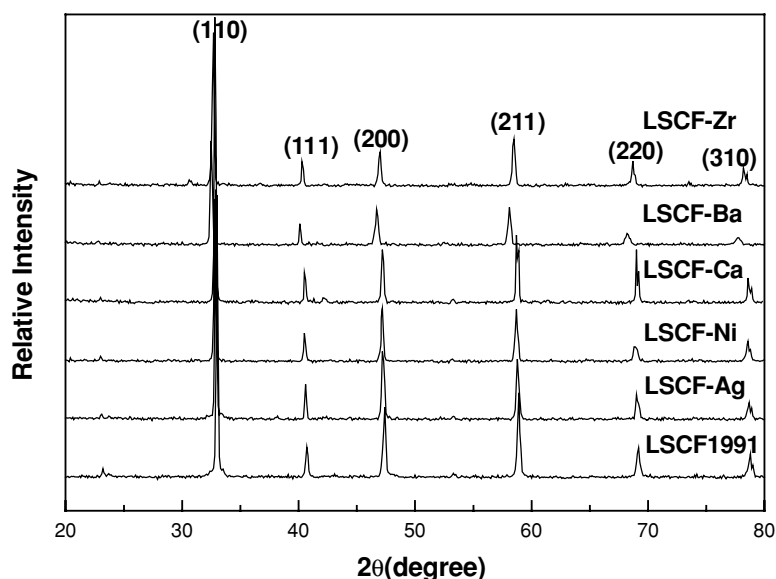
membranes (Shao et al., 2001; Yang et al., 2003a, 2003b). Yamazoe and co workers (Kusaba et al., 2000; Kusaba et al., 2002b) found that 10–20% partial substitution of the metal ion in the A-site of $\text{SrCo}_{0.9}\text{Fe}_{0.1}$ by Ca^{2+} was effective to maintain its perovskite type structure. The present study was focused on examining the effects of doping Ag^+ , Ni^{2+} , Ca^{2+} , Ba^{2+} , and Zr^{4+} in perovskite-type oxide $\text{La}_{0.1}\text{Sr}_{0.9}\text{Co}_{0.9}\text{Fe}_{0.1}\text{O}_{3-\delta}$ on its oxygen sorption properties. Our main objective was to study the doping method for improving oxygen sorption and desorption rate of the perovskite type metal oxide sorbent for applications in the high temperature sorption process for air separation.

2 Experimental

Powders of pure $\text{La}_{0.1}\text{Sr}_{0.9}\text{Co}_{0.9}\text{Fe}_{0.1}\text{O}_{3-\delta}$ (LSCF-1991), and Ag^+ , Ni^{2+} , Ca^{2+} , Ba^{2+} and Zr^{4+} -doped $\text{La}_{0.1}\text{Sr}_{0.9}\text{Co}_{0.9}\text{Fe}_{0.1}\text{O}_{3-\delta}$ (abbreviated as LSCF-Ag, LSCF-Ni, LSCF-Ca, LSCF-Ba and LSCF-Zr respectively) were synthesized by the liquid citrate method from the corresponding metal nitrates. Nitrates of La, Sr, Co, Fe in stoichiometric portions, and the nitrate of one dopant metal (5% molar ratio to LSCF1991) were dissolved in de-ionized water. 50% excessive citrate acid was added into the solution to allow polymerization at 100°C for 4 h and condensation at 110°C for 4 h. After condensation, the gel-like brick red product was dried at 110°C for hrs and self ignited at 420°C for 30 min to burn out the organic compounds in the material. The powder was then sintered at 1250°C for 20 h with a ramping rate of 60°C/h to obtain the perovskite structure.

The phase structure of the prepared samples in air was examined by XRD (Siemens D-50, Cu $K_{\alpha 1}$ radiation). To study the phase structure of the samples in reducing oxygen atmosphere, the powders were first annealed at 700°C for 5 h in He flow, quenched down to room temperature in the same atmosphere, and then removed and examined in air by XRD immediately. The phase structure stability of the samples in He flow was studied by simultaneous TGA/DSC (TA Instruments, SDT2960) analysis. During measurements, helium was introduced into the sample zone at the flow rate of 100 ml/min. Heat flux and weight change were recorded when samples were heated up from the room temperature to 950°C, with a ramping rate of 10°C/min.

Fig. 1 XRD patterns of LSCF1991, LSCF-Ag, LSCF-Ni, LSCF-Ca, LSCF-Ba and LSCF-Zr powders sintered at 1250°C



Kinetics and oxygen equilibrium of oxygen sorption and desorption process for these samples were measured by TGA instrument (TA Instruments, SDT2960). Oxygen sorption/desorption process started when the sample experienced a sudden increase/decrease in oxygen activity of the gas stream passing through the sample compartment at a given temperature. In the measurements, about 50 mg of sample powders were placed in the alumina sample holder and the sample compartment was heated to 110°C to remove the water moisture till a stable weight was achieved. The sample was then heated to the desired temperature, for example, 600°C, in He flow ($P_{O_2} = 0.0001$ atm). Sample was kept isothermally until a stable weight was observed. The feed gas was quickly switched from He to dry air ($P_{O_2} = 0.21$ atm) to initiate the oxygen sorption process. The corresponding weight change was recorded automatically by the TGA instrument. Sub-

sequently, the kinetics during the desorption process was also measured for the same sample subjected to a change of the surrounding gas from air to He.

3 Results and discussion

XRD patterns of the as-synthesized LSCF1991, LSCF-Ag, LSCF-Ca, LSCF-Ba, LSCF-Ni and LSCF-Zr oxides (all with 5 molar% dopant) are shown in Fig. 1. All doped-oxides have the similar XRD patterns of perovskite structure with diffraction peaks for the doped-oxides shifted slightly to the left, as compared to undoped LSCF1991. The small phase with the distinct diffraction peak at about 30° for LSCF-Zr oxides is identified as ZrO_2 .

Table 1 lists both lattice parameters of the samples shown in Fig. 1 and the radii of the doping ions. The

Table 1 Lattice parameters of prepared samples in air and radii of the doping ions

Oxides	Lattice parameters (Å)	Ions	Ionic radii (Å)
LSCF1991	3.837	La^{3+}	1.36
		Sr^{2+}	1.44
		Co^{2+}/Co^{3+}	0.65/0.545
		Fe^{3+}	0.55
LSCF-Ag	3.846	Ag^{+}	1.40
LSCF-Ni	3.847	Ni^{2+}	0.67
LSCF-Ca	3.838	Ca^{2+}	1.34
LSCF-Ba	3.885	Ba^{2+}	1.62
LSCF-Zr	3.863	Zr^{4+}	0.72

lattice parameters were calculated from the d -values of the characteristic peaks for the (110), (111), (200), (220) and (310) planes. The lattice parameters for all the doped samples are larger than the undoped one, even for the dopants with a size smaller than hosting ions in the A-site (Sr^{2+} and La^{3+}), as shown in Table 1. These results suggest that the doped ion may have substituted the metal ion at A-site, like Ag^+ , Ca^{2+} and Ba^{2+} , or at B site, like Ni^{2+} and Zr^{4+} , and it may also present at the interstitial position in the lattice. The unit cell must expand to accommodate the doped ions. Wiik and co workers (Faaland et al., 1999; Wiik et al., 1999) also found that the lattice of $\text{La}_{0.7}\text{Sr}_{0.3}\text{MnO}_3$ expanded after being doped with Zr^{4+} .

Oxygen sorption capacity is defined here as the equilibrium amount of oxygen taken up by a perovskite-type oxide after the surrounding atmosphere changes from helium to air. It can be determined from the oxygen nonstoichiometry of the perovskite-type oxide by:

$$q = -\frac{\delta(\text{air}) - \delta(\text{He})}{2M_w} \quad (2)$$

where $\delta(\text{He})$ and $\delta(\text{Air})$ are respectively the oxygen nonstoichiometry of the perovskite type oxide in He and air and M_w is the average molecular weight of the sample. The oxygen nonstoichiometry $\delta(\text{He})$ and $\delta(\text{Air})$ at various temperatures were determined from TGA measurements (Yang et al., 2002). The results of the oxygen sorption capacity for the samples at various temperatures are shown in Fig. 2.

As can be seen from Fig. 2, the oxygen sorption capacities of the samples decrease in the order: $\text{LSCF1991} > \text{LSCF-Ag} > \text{LSCF-Ni} > \text{LSCF-Ca} > \text{LSCF-Ba} > \text{LSCF-Zr}$. Doping Ba^{2+} and Zr^{4+} into the LSCF1991 significantly decreases its oxygen sorption capacity. The measured sorption capacity on these two samples increases with increasing temperature in the temperature range of 700–900°C. Doping other ions (Ag, Ni and Ca) also decreases oxygen sorption capacity but the effects are less significant. The oxygen sorption capacity of these samples and LSCF1991 decreases with increasing temperature. These differences in temperature dependency and oxygen sorption capacity reduction for various doping ions are explained next.

For oxygen sorption on perovskite-type metal oxides it is oxygen nonstoichiometry, δ , not the oxygen sorption capacity, that is a function of the oxygen partial pressure and temperature, i.e., $\delta = f(P_{\text{O}_2}, T)$. As indicated by Eq. (2), the oxygen sorption capacity corresponds to the difference of δ in the perovskite-type sorbent between the state at $P_{\text{O}_2} = 0.21$ atm (oxygen partial pressure in air at 1 atm) and $P_{\text{O}_2} = 0.0001$ atm (determined by oxygen impurity in He at 1 atm). Perovskite type metal oxides may transform from the disordered perovskite structure to an ordered brownmillerite structure with decreasing oxygen partial pressure at lower temperature range (Yang and Lin, 2005). For perovskite type metal oxides without the disorder to order phase transition, the oxygen nonstoichiometry increases with increasing temperature in both He and

Fig. 2 Comparison of oxygen sorption capacity of LSCF1991, LSCF-Ag, LSCF-Ni, LSCF-Ca, LSCF-Ba and LSCF-Zr at different temperatures

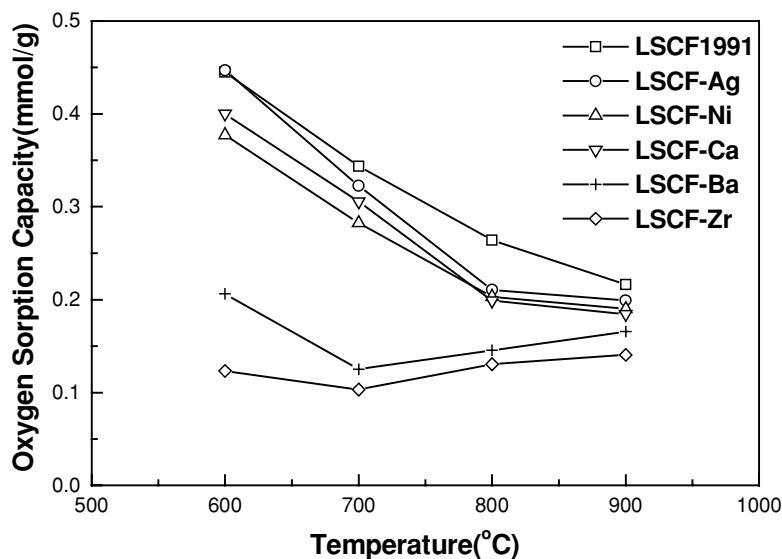
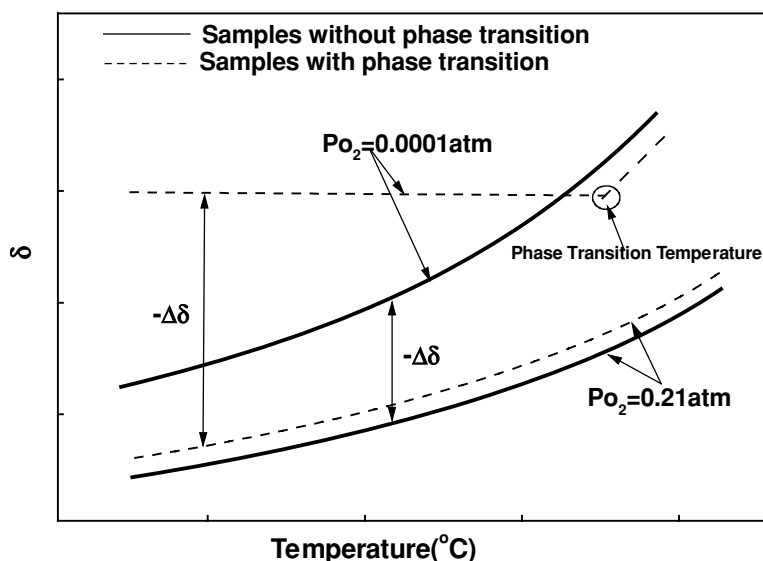


Fig. 3 Schematic description of the difference in oxygen storage capacity between materials with and without a phase transition



air, with the degree of increase in He higher than in air (Mizusaki et al., 1985, 1989; Sitte et al., 2002). These are shown by the two solid curves in Fig. 3. In these cases, the oxygen sorption capacity ($-\Delta\delta$) of the material also increases with temperature, as shown in Fig. 3.

The dashed curves in Fig. 3 show oxygen nonstoichiometry for the perovskite type metal oxides which can transfer from the perovskite structure with disordered oxygen vacancy to the brownmillerite structure ($A_2B_2O_5$) with an increased number of oxygen sites being vacant and ordered when oxygen partial pressure or temperature decreases (Kruidhof et al., 1993; Qiu et al.,

1995). For these materials at low oxygen partial pressure (e.g., 0.0001 atm) and in a specific temperature range, their equilibrium state is in the ordered brownmillerite structure whose oxygen nonstoichiometry is essentially independent of temperature. This is illustrated by the section of the horizontal dashed line in Fig. 3. Obviously, ($-\Delta\delta$) between the two dashed curves for these samples may decrease and, after reaching a minimum, increase with increasing temperature, as shown in Fig. 3.

The phase structure and disorder to order phase transition of all the samples in He were studied by XRD and TGA/DSC. Figure 4 shows the XRD patterns of the

Fig. 4 XRD patterns of LSCF1991, LSCF-Ag, LSCF-Ni, LSCF-Ca, LSCF-Ba and LSCF-Zr powder annealed at 700°C for 5 h in helium

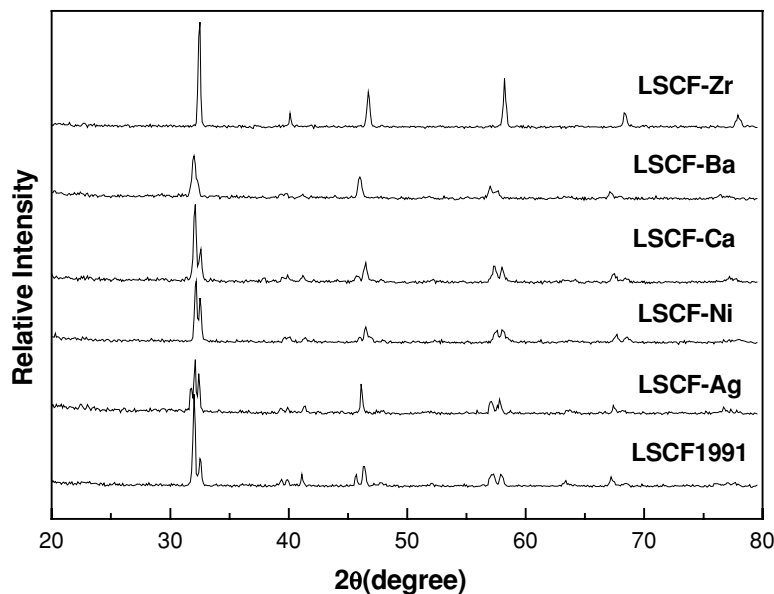
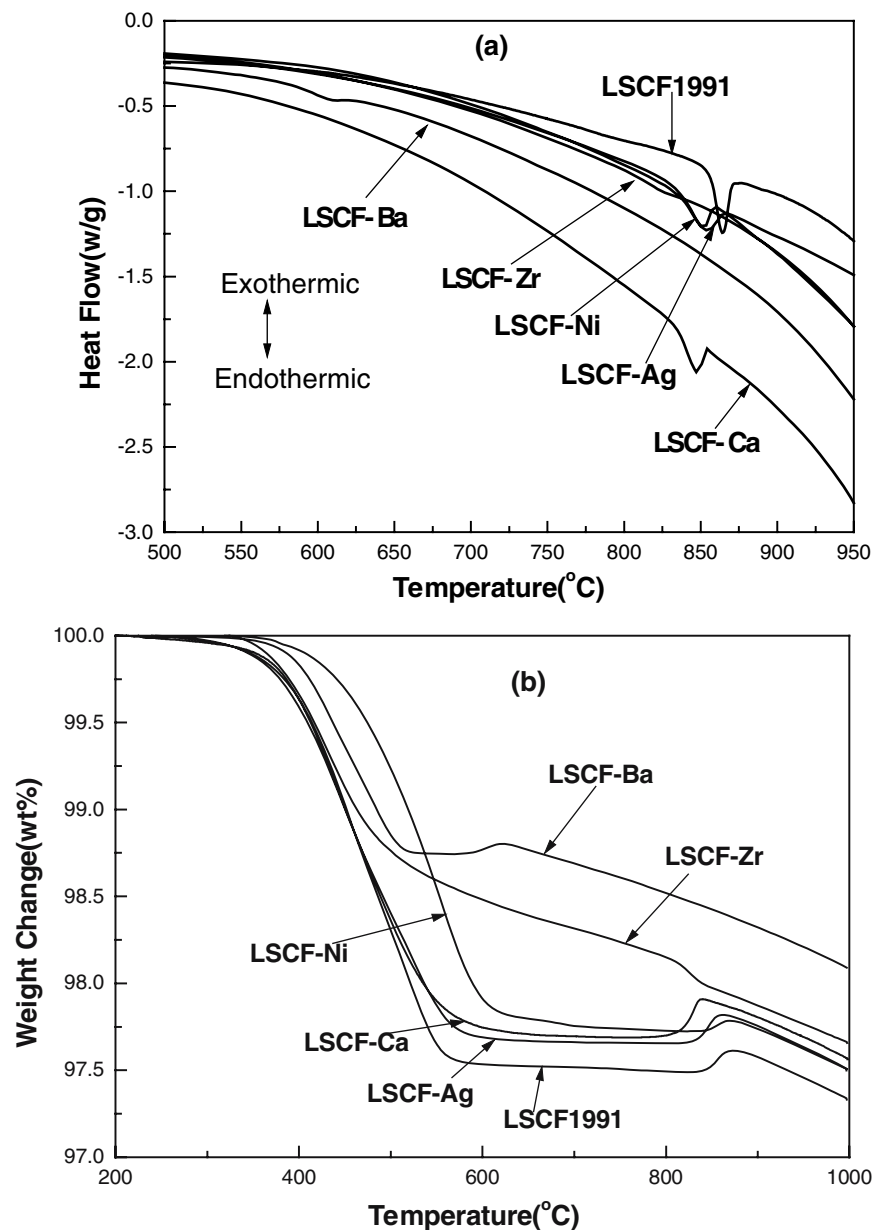


Fig. 5 DSC (a) and TG (b) curves of LSCF1991, LSCF-Ag, LSCF-Ni, LSCF-Ca, LSCF-Ba and LSCF-Zr oxides in helium during heating process (10°C/min)



LSCF1991, LSCF-Ag, LSCF-Ni, LSCF-Ca, LSCF-Ba and LSCF-Zr powders quenched down from 700°C to room temperature in He. The phase is considered stable if the characteristic diffraction peaks of the perovskite phase are well maintained. For LSCF1991, LSCF-Ag, LSCF-Ni and LSCF-Ca, the main diffraction peaks are split and the degree of the splits for the doped samples is similar to that for LSCF1991. The splits indicate that the phase structure of the powders has already changed from perovskite to brownmillerite in He at 700°C

(Kusaba et al., 2002a). The XRD patterns for LSCF-Ba show only slight split in (111) and (220), which indicates that the portion of crystalline with brownmillerite structure is quite low in the whole samples. LSCF-Zr do not exhibit such splits.

Figure 5(a) shows the DSC curves of LSCF1991, LSCF-Ag, LSCF-Ni, LSCF-Ca, LSCF-Ba and LSCF-Zr heated in He. As shown in the figure, except for LSCF-Ba and LSCF-Zr, all of the other oxides have an endothermic peak at round 860°C in the DSC curves.

For LSCF-Ba, there is a very small endothermic peak at round 600°C. The endothermic peak is attributed to the phase transition from the ordered brownmillerite phase to the disordered perovskite phase. The TG results are shown in Fig. 5(b). The phase transition from perovskite phase to brownmillerite phase can generally be recognized by the appearance of a plateau.

The phase transition temperature and the height of the phase transition peak in DSC curves, as well as the width of the plateau in TG curves can be used to determine the degree of the tendency for disorder to order phase transition (Yamamura et al., 1998). Materials with higher phase transition temperature or phase transition peak, and broader plateau have the higher tendency for the phase transition from the perovskite structure to brownmillerite structure in He as temperature decreases, as summarized in Table 2. The results show that the tendency for phase transition from perovskite structure to brownmillerite structure in He for the samples studied decrease in the order: LSCF > LSCF-Ag > LSCF-Ni > LSCF-Ca > LSCF-Ba > LSCF-Zr. This is consistent with the order of the oxygen sorption capacity for the materials. The results in Table 2 confirm the phase transition effects on oxygen sorption capacity illustrated in Fig. 3. For example, for samples LSCF, LSCF-Ag, LSCF-Ni, and LSCF-Ca, the oxygen sorption capacity decreases with increasing temperature in the range of 600–900°C due to their phase transition temperatures from brownmillerite to perovskite in He are at around 850°C. For LSCF-Ba with a phase transition temperature at around 603°C, it shows a decrease of oxygen sorption capacity in 600–700°C followed by an increase in 700–900°C with increasing temperature. For LSCF-Zr without phase transition, theoretically the oxygen sorption capacity increases with increasing temperature, the slight decrease of oxygen sorption capacity at 700°C may result from the experimental error. The

results confirm that doping ions of different size into perovskite type metal oxides can have much effect on the phase stability and oxygen sorption capacity of the materials.

Figure 6 shows the adsorption (a) and desorption (b) kinetics of samples at 600°C. The adsorption rate for all the samples are similar and fast, as shown in Fig. 6(a). In this study we only focused on the desorption kinetics. A typical oxygen desorption process may include the following three steps: (1) Diffusion of oxygen ions or vacancies and electrons in the bulk of the crystallite; (2) Charge transfer reactions on the crystallite surface, $\text{O}_\text{O}^\times + 2\dot{h} \Leftrightarrow \dot{\text{V}}_\text{O} + \frac{1}{2}\text{O}_2$; (3). Transport of an oxygen molecule through a grain boundary. Zeng and Lin (1998) studied kinetics of oxygen sorption into and desorption from the LSCF particles by the TGA method. They suggested the step of surface exchange as the rate-limiting for oxygen transport in the LSCF particles with sizes in the micron range. A linear driving force model was used to derive the relationship between normalized weight change and the surface reaction constants as follow (Zeng and Lin, 1998):

$$\frac{w(t) - w(e)}{w(0) - w(e)} = \exp(-2\phi kt) \quad (3)$$

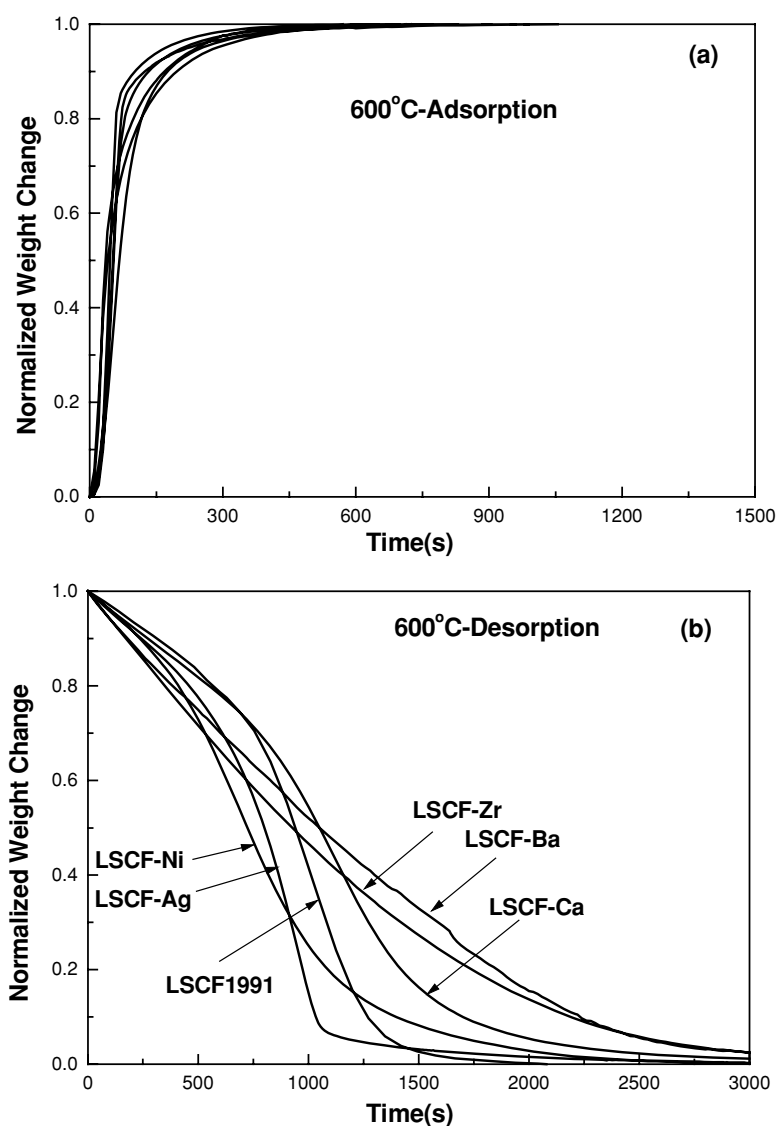
where $w(0)$, $w(e)$ and $w(t)$ are respectively the initial (in air), equilibrium (in helium) and instant weight of the sample. k is the surface reaction rate constant and Φ is the geometry factor of $\Phi = 6/D$ (D is the crystalline size of the sample). Since all the doped oxides were prepared and treated under the same conditions, the difference in the geometry factors for all the samples is negligible. Therefore, the difference in the kinetic curves at the same temperature reflects the difference in the surface reaction rate constants.

As shown from Fig. 6(b), the desorption rate for the samples at 600°C decreases in the order: LSCF-Ag

Table 2 Results of phase transition in the samples from DSC/TG curves

Oxides	Phase transition temperature in DSC curves (°C)	Height of the phase transition peak in DSC curves (w/g)	Width of the plateau plateau in TG curves (°C)
LSCF1991	864	0.91–1.24	582–856
LSCF-Ag	853	1.05–1.22	592–820
LSCF-Ni	850	1.02–1.20	643–843
LSCF-Ca	847	1.92–2.04	614–800
LSCF-Ba	603	0.42–0.47	522–592
LSCF-Zr	/	/	/

Fig. 6 Comparison of adsorption (a) and desorption kinetics (b) of LSCF1991, LSCF-Ag, LSCF-Ni, LSCF-Ca, LSCF-Ba and LSCF-Zr at 600°C



> LSCF-Ni > LSCF1991 > LSCF-Ca > LSCF-Zr > LSCF-Ba. The same trend of desorption kinetics is found for these samples in the temperature range of 600–800°C. Except for LSCF and LSCF-Ba, this order is the same as for the tendency for disorder to order phase transition (i.e., LSCF > LSCF-Ag > LSCF-Ni > LSCF-Ca > LSCF-Ba > LSCF-Zr). The process of oxygen desorption (with oxygen partial pressure decrease) is accompanied with phase transition from the perovskite to brownmillerite structure for the same samples. This suggests that such phase transition also enhances the oxygen desorption rate. The detailed

study of the effects of phase transition on oxygen sorption and desorption kinetics is now under investigation in our group. Doping Ag^+ and Ni^{2+} may provide additional effects which enhance surface reaction rate (Ni^{2+} and Ag^+ have been used as catalyst to modify the surface of perovskite-type oxides for complete combustion of methane (Tikhonovich et al., 1998; Wang et al., 2000)). This could be the reason for the faster oxygen desorption rate for the Ag^+ and Ni^{2+} doped samples as compared to LSCF1991. The slowest desorption rate for LSCF-Ba may due to the large binding energy of metal ions and oxygen molecular.

4 Conclusions

$\text{La}_{0.1}\text{Sr}_{0.9}\text{Co}_{0.9}\text{Fe}_{0.1}\text{O}_{3-\delta}$ can be doped with 5% Ag^+ , Ni^{2+} , Ca^{2+} , Ba^{2+} or Zr^{4+} . The dopant appears to be dissolved totally into the LSCF1991 matrix causing lattice expansion. The tendency for phase transition from the disordered perovskite structure to the ordered brownmillerite structure in He decreases in the order of $\text{LSCF1991} > \text{LSCF-Ag} > \text{LSCF-Ni} > \text{LSCF-Ca} > \text{LSCF-Ba} > \text{LSCF-Zr}$, consistent with the order of the oxygen sorption capacity for these samples. Except for LSCF and LSCF-Ba, the oxygen desorption rate also decreases in almost the same order for the doped samples. Doping increases the tendency of the disorder to order phase transition and enhances oxygen desorption rate during the oxygen desorption step. Doping Ag^+ and Ni^+ provide more pronounced enhancement in oxygen desorption rate due properly due their additional catalytic properties promoting oxygen surface reaction.

Acknowledgments The work was supported by U.S. National Science Foundation (CTS-0132694).

References

- Choudhary, V.R., B.S. Uphade, and S.G. Pataskar, "Low Temperature Complete Combustion of Methane over Ag-doped LaFeO_3 and $\text{LaFe}_{0.5}\text{Co}_{0.5}\text{O}_3$ Perovskite Oxide Catalysts," *Fuel*, **78**, 919–921 (1999).
- Dyer, P.N., R.E. Richards, S.L. Russek, and D.M. Taylor, "Ion Transport Membrane Technology for Oxygen Separation and Syngas Production," *Solid State Ionics*, **134**, 21–33 (2000).
- Faaland, S., M.A. Einarsrud, K. Wiik, and T. Grande, "Reactions between $\text{La}_{1-x}\text{Ca}_x\text{MnO}_3$ and CaO -stabilized ZrO_2 —Part I—Powder Mixtures," *J. Mater. Sci.*, **34**, 957–966 (1999).
- Figueiredo, F.M., V.V. Kharton, A.P. Viskup, and J.R. Frade, "Surface Enhanced Oxygen Permeation in $\text{CaTi}_{1-x}\text{Fe}_x\text{O}_{3-\delta}$ Ceramic Membranes," *J. Membr. Sci.*, **236**, 73–80 (2004).
- Kang, D., S. Srinivasan, R.M. Rhorogood, and E.P. Foster, "Integrated High Temperature Method for Oxygen Production," US Patent 5 516 359 (1996).
- Kharton, V.V., A. Kovalevsky, A.A. Yaremchenko, F.M. Figueiredo, E.N. Naumovich, A.L. Shaulo, and F.M.B. Marques, "Surface Modification of $\text{La}_{0.3}\text{Sr}_{0.7}\text{CoO}_{3-\delta}$ Ceramic Membranes," *J. Membr. Sci.*, **195**, 277–287 (2002).
- Kharton, V.V., A.A. Yaremchenko, E.V. Tsipis, A.A. Valente, M.V. Patrakeev, A.L. Shaula, J.R. Frade, and J. Rocha, "Characterization of Mixed-Conducting $\text{La}_2\text{Ni}_{0.9}\text{Co}_{0.1}\text{O}_{4+\delta}$ Membranes for Dry Methane Oxidation," *Appl. Catal. A*, **261**, 25–35 (2004).
- Kruidhof, H., H.J.M. Bouwmeester, R.H.E. Vondorn, and A.J. Burggraaf, "Influence of Order-Disorder Transitions on Oxygen Permeability through Selected Nonstoichiometric Perovskite-Type Oxides," *Solid State Ionics*, **63–65**, 816–822 (1993).
- Kusaba, H., G. Sakai, N. Miura, and N. Yamazoe, "Oxygen Permeability and Phase Transformation of Strontium-cobaltite System. Effect of B-site Substitution," *Electrochem.*, **68**, 409–411 (2000).
- Kusaba, H., G. Sakai, K. Shimano, N. Miura, and N. Yamazoe, "Oxygen-sorptive and -Desorptive Properties of Perovskite-related Oxides under Temperature-swing Conditions for Oxygen Enrichment," *Solid State Ionics*, **152**, 689–694 (2002a).
- Kusaba, H., G. Sakai, K. Shimano, N. Yamazoe, and N. Miura, "Temperature-swing Based Oxygen Enrichment by using Perovskite-type Oxides," *J. Mater. Sci. Lett.*, **21**, 407–409 (2002b).
- Lin, Y.S., D.L. McLean, and Y. Zeng, "High Temperature Adsorption Process," US Patent 6 059 858 (2000).
- Mizusaki, J., S. Yamauchi, K. Fueki, and A. Ishikawa, "Nonstoichiometry of the Perovskite-Type Oxide $\text{La}_{1-x}\text{Sr}_x\text{CoO}_{3-\Delta}$," *Solid State Ionics*, **12**, 119–124 (1984).
- Mizusaki, J., M. Yoshihiro, S. Yamauchi, and K. Fueki, "Nonstoichiometry and Defect Structure of the Perovskite-type Oxides $\text{La}_{1-x}\text{Sr}_x\text{FeO}_{3-\Delta}$," *J. Solid State Chem.*, **58**, 257–266 (1985).
- Mizusaki, J., Y. Mima, S. Yamauchi, K. Fueki, and H. Tagawa, "Nonstoichiometry of the Perovskite-type Oxides $\text{La}_{1-x}\text{Sr}_x\text{CoO}_{3-\Omega}$," *J. Solid State Chem.*, **80**, 102–111 (1989).
- Prasad, R., "Advanced Membrane System for Separating Gaseous Mixtures," US Patent 5 709 732 (1998).
- Qiu, L., T.H. Lee, L.M. Liu, Y.L. Yang, and A.J. Jacobson, "Oxygen Permeation Studies of $\text{SrCo}_{0.8}\text{Fe}_{0.2}\text{O}_{3-\Delta}$," *Solid State Ionics*, **76**, 321–329 (1995).
- Shao, Z.P., G.X. Xiong, J.H. Tong, H. Dong, and W.S. Yang, "Ba Effect in Doped $\text{SrCo}_{0.8}\text{Fe}_{0.2}\text{O}_{3-\delta}$ on the Phase Structure and Oxygen Permeation Properties of the Dense Ceramic Membranes," *Sep. Purif. Technol.*, **25**, 419–429 (2001).
- Sitte, W., E. Bucher, and W. Preis, "Nonstoichiometry and Transport Properties of Strontium-Substituted Lanthanum Cobaltites," *Solid State Ionics*, **154**, 517–522 (2002).
- Tan, L., L. Yang, X.H. Gu, W.Q. Jin, L.X. Zhang, and N.P. Xu, "Structure and Oxygen Permeability of Ag-doped $\text{SrCo}_{0.8}\text{Fe}_{0.2}\text{O}_{3-\delta}$ Oxides," *AIChE J.*, **50**, 701–707 (2004a).
- Tan, L., L. Yang, X.H. Gu, W.Q. Jin, L.X. Zhang, and N.P. Xu, "Influence of the Size of Doping Ion on Phase Stability and Oxygen Permeability of $\text{SrCo}_{0.8}\text{Fe}_{0.2}\text{O}_{3-\delta}$ Oxide," *J. Membr. Sci.*, **230**, 21–27 (2004b).
- Tikhonovich, V.N., V.V. Kharton, E.N. Naumovich and A.A. Savitsky, "Surface Modification of $\text{La}(\text{Sr})\text{MnO}_3$ Electrodes," *Solid State Ionics*, **106**, 197–206 (1998).
- Wang, W., G.D. Lin, H.B. Zhang, and Z.T. Xiong, "Ag/ $\text{La}_{0.6}\text{Sr}_{0.4}\text{MnO}_3$ Catalysts for Deep Oxidation of CH_4 and CH_3OH at Low Concentrations," *Acta Physico-Chimica Sinica*, **16**, 299–306 (2000).
- Wiik, K., C.R. Schmidt, S. Faaland, S. Shamsili, M.A. Einarsrud, and T. Grande, "Reactions between Strontium-substituted Lanthanum Manganite and Yttria-stabilized Zirconia: I, Powder Samples," *J. Am. Ceram. Soc.*, **82**, 721–728 (1999).

- Yamamura, H., Y. Yamada, T. Mori, and T. Atake, "Order-Disorder Transition of Oxygen Vacancy in the Brownmillerite System," *Solid State Ionics*, **108**, 377–381 (1998).
- Yang, L., X.H. Gu, L. Tan, L.X. Zhang, C.Q. Wang, and N.P. Xu, "Role of ZrO_2 Addition on Oxygen Transport and Stability of ZrO_2 -promoted $\text{SrCo}_{0.4}\text{Fe}_{0.6}\text{O}_{3-\delta}$," *Sep. Purif. Technol.*, **32**, 301–306 (2003a).
- Yang, L., L. Tan, X.H. Gu, H. Qi, W.Q. Jin, L.X. Zhang, and N.P. Xu, "Effect of the Size and Amount of ZrO_2 Addition on Properties of $\text{SrCo}_{0.4}\text{Fe}_{0.6}\text{O}_{3-\delta}$," *AIChE J.*, **49**, 2374–2382 (2003b).
- Yang, Z.H., Y.S. Lin, and Y. Zeng, "High-temperature Sorption Process for Air Separation and Oxygen Removal," *Ind. Eng. Chem. Res.*, **41**, 2775–2784 (2002).
- Yang, Z.H. and Y.S. Lin, "Equilibrium of Oxygen Sorption on Perovskite-type Lanthanum Cobaltite Sorbent," *AIChE J.*, **49**, 793–798 (2003a).
- Yang, Z.H. and Y.S. Lin, "High-Temperature Oxygen Sorption in a Fixed Bed Packed with Perovskite-type Ceramic Sorbents," *Ind. Eng. Chem. Res.*, **42**, 4376–4381 (2003b).
- Yang, Z.H. and Y.S. Lin, "Synergetic Thermal Effects for Oxygen Sorption and Order-disorder Transition on Perovskite-type Oxides," *Solid State Ionics*, **176**, 89–96 (2005).
- Zeng, Y. and Y.S. Lin, "A Transient TGA Study on Oxygen Permeation Properties of Perovskite-Type Ceramic Membrane," *Solid State Ionics*, **110**, 209–221 (1998).